# Improving the formability of sandwich sheets by the hydrostatic effect of encapsulated media

Yuki Shibuya[1] · Jun Yanagimoto[1]

## Abstract

Various sandwich structures have been developed as lightweight structures. They have excellent specific stiffness owing to their low density. However, owing to the existence of various failure modes, which are classified into core shear failure, tensile fracture of the face sheet, buckling of the face sheet, and delamination, it is difficult to deform sandwich sheets without any failure. A new forming strategy was proposed in this study. Buckling of the face sheet during drawing was suppressed by filling the encapsulated media in a 3D core between the face sheets to exploit its hydrostatic effect. This process is similar to the freeze-bend method, in which the pipe is filled with ice during bending to suppress wrinkles and flattening. Ice, wax, and low-melting alloys were used as the encapsulated media, and their formability and ease of removal were investigated. Further, a shear strength test was performed on the specimens that were cut out from the drawn products to evaluate failure during forming. Based on these experimental results, the characteristics required for the encapsulated media were summarized.

## Introduction

To avoid deterioration of the global environment, such as global warming, it is effective to lighten structural materials to reduce greenhouse gas emissions. A reduction in the energy consumption also leads to lower operating costs. Lightweight materials are also required in the development of new transportation such as flying cars [1].

Weight reduction methods can be classified into two groups. One is the replacement method, which uses materials with lower densities than those previously used [2]. Carbon fiber-reinforced plastic (CFRP) has been studied as such material [3, 4]. However, it is often necessary to change the structure based on the changes in the strength and stiffness of the material to maintain a safe level [5]. The other method is structural optimization, in which the same properties are obtained with less material using computational methods [6, 7].

One solution for weight reduction is by use of a sandwich structure, which consists of face sheets attached to a 3D core, as shown in Fig. 1 [8, 9].

The specific stiffness of sandwich structure is higher than that of fiber metal laminate (FML), and it is also plastically deformable. However, the defects during forming limits the degree of forming. The defects are classified into core shear failure, tensile fracture of face sheet, buckling of face sheet, and delamination, and they have been studied to enhance the formability [10-13]. Owing to the complex mode of failure, sandwich sheets are hard-to-form sheets, such that complex structures are usually produced by separately forming the face sheets and core before joining [14]. Alternatively, additive manufacturing is applied to manufacture the sheets [15]. If the flat sandwich sheet can be plastically deformed into the desired geometry without failure, it will result in marked decrease in processing time and cost and increase in the usage as structural material.

A new solution for the forming process to improve the formability was proposed and investigated in this study. The proposed method utilizes the encapsulated media and its hydrostatic effect to effectively constrain the face sheet to avoid wrinkles and failures, and wrinkle-free spheres can be drawn from the flat sandwich sheets using the proposed method.

✉ Yuki Shibuya
  yuki.shibuya.ut@gmail.com

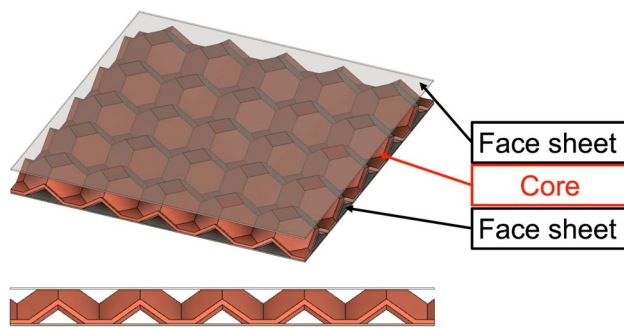1 Department of Mechanical Engineering, The University of Tokyo, Tokyo, Japan
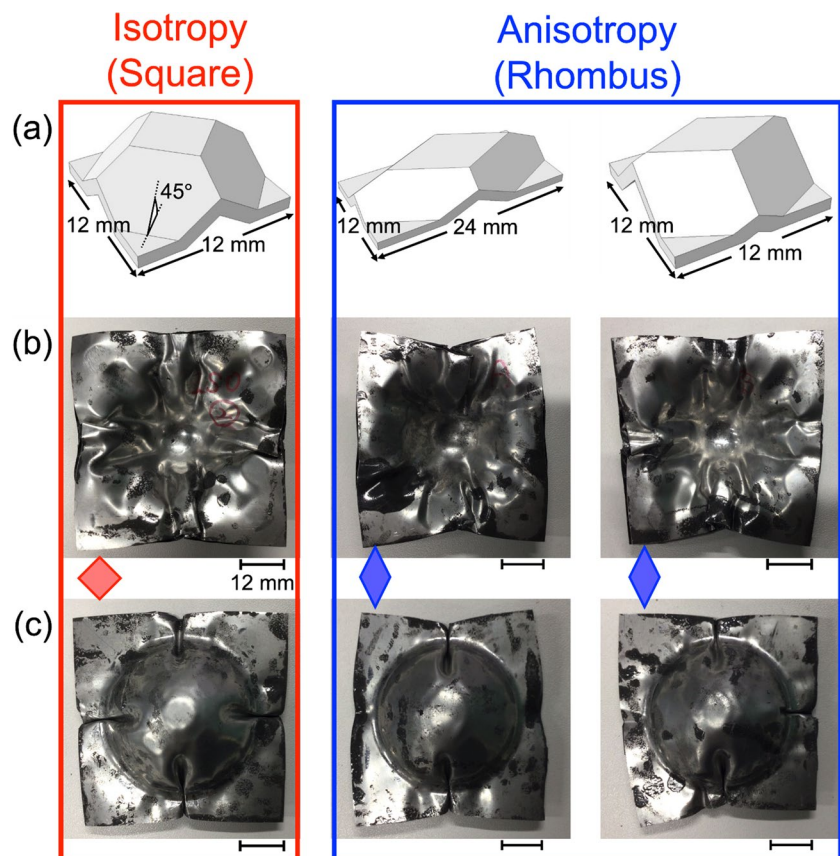
**Fig. 1** Sandwich sheet

## Method

### Forming of sandwich sheet

3D cores enable the creation of sheets with a wide range of mechanical properties and anisotropy; however, the most crucial drawback is that face sheets can buckle inward during drawing, even if a block holding plate is used. Many wrinkles occur during drawing when a previously published structure is applied, whose core has square or rhombus unevenness, as shown in Fig. 2 [16].

In the case of sandwich sheets with a square dome core, large wrinkles occur in two directions. Owing to the anisotropy of the rhombic core, sandwich sheets with rhombic cores have wrinkles in one direction.

The freeze-bend method has been used to bend double pipes [17]. This is a method of filling the pipe with ice during deformation and applying internal pressure, suppressing the flattening and wrinkling of pipes during bending. The freeze-bend method can be extended to the secondary formation of sandwich sheets. The sandwich sheets are filled with ice, wax, and fusible alloys during drawing. Fusible alloys are used to hold fragile components [18].

The proposed process is illustrated schematically in Fig. 3. The encapsulated media suppresses the failure of the face sheet and core owing to the hydrostatic effect. These materials can be reused, as illustrated in Fig. 3.

### Sandwich structure

As shown in Fig. 2, square/rhombic periodic domes, which have been proposed to exhibit excellent bending rigidity, were used for the core [16]. The period length was 12 mm and the specimen size for drawing was 62 mm square. To manufacture the cores, six layers of unidirectional long-fiber CFRP prepreg (Toray P3252S-10, thickness 0.1 mm)

**Fig. 2** Wrinkles after drawing of sandwich sheet with square or rhombus core. **a** Periodic shape of the core, **b** Top view (punch side), **c** Bottom view (die side)

**Fig. 3** Process of forming with encapsulated media
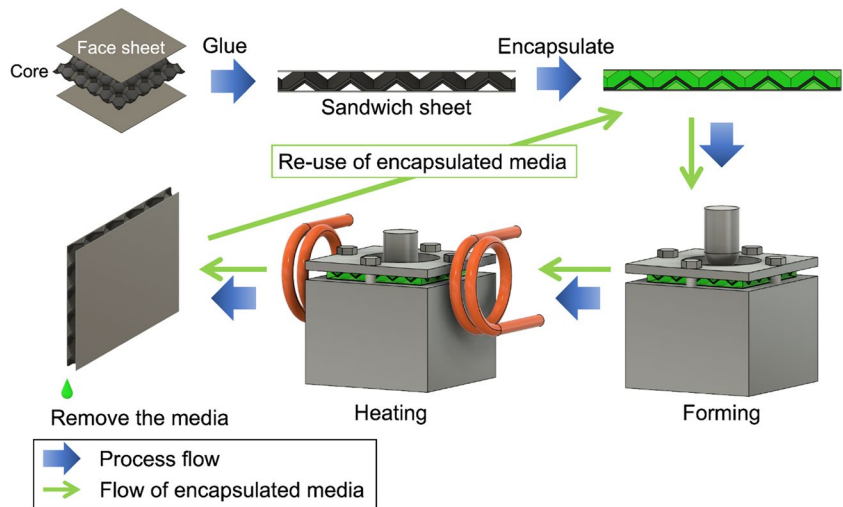


**Table 1** Properties of encapsulated media

|  | Water (Ice) | Wax | Fusible alloy |
|---|---|---|---|
| Density in solid [g/cm$^3$] | 0.92 | 0.92 | $8.69 \times 10^3$ |
| Melting point [°C] | 0 | 117 | 78 |
| Velocity in liquid [cPs] | 0.55 (50 °C) | 1560 (149 °C) |  |

laminated with [0/+60/-60]$_s$ were deformed using resin molds (polycarbonate) and solidified in an autoclave. The core thickness was 0.6 mm and the apparent thickness of the 3D core was 5 mm. SUS304 0.3 mm plates were used for face sheets and glued to a core with one liquid-type adhesive IW2460 (3 M Company). The total thickness of the sandwich sheet was 5.6 mm.

## Experimental procedure

The materials for the encapsulated media to fill in the core between face sheets were selected as tap water ice, Ferris green wax (Freeman Manufacturing & Supply Company), and fusible U-alloy (OSAKA ASAHI CO., LTD.). The material properties are listed in Table 1.

The materials used for the encapsulated media were divided into two groups according to the difference in volume change during solidification, and a suitable filling method was used for each material.

a)   Water (volume increase in solidification)

   a-1) Submerge the entire sandwich sheet into the water. The amount of volume expansion during freezing can leak into the surroundings.
   a-2) Freeze.
   a-3) Crack and remove excess ice.

b)   Wax / Fusible alloy (volume decrease in solidification)

   b-1) Close three edges with tape and extend the remaining edge. This spout compensates for the volume reduction during solidification.
   b-2) Melt the material for encapsulation.
   b-3) Pour the melting material into the specimens and vibrate them until bubbles do not appear.
   b-4) Solidify with slow cooling to prevent voids.
   b-5) Remove the tape and cut off the excess material.

After the media were encapsulated, drawing experiments were conducted to validate the formability of the sandwich sheets. The experimental setup for the drawing is shown in Fig. 4.

The die was fixed, and the specimen was fixed between the die and blank holder using four bolts. Forming was performed using a punch velocity of 0.1 mm/s with a THERMECMASTOR-Z (Fuji Electronic Industrial Co., Ltd). The induction coil is shown in Fig. 4, but the drawing experiment was conducted at room temperature. After drawing, the specimens were heated, and the encapsulated materials were melted before unloading to suppress separation on the adhesive surface owing to the elastic recovery force of the encapsulated media, as illustrated in Fig. 3.

The shear strengths of the products were measured to evaluate their properties. As shown in Fig. 5, the specimen drawn with the fusible alloy was cut out with a width of one period (12 mm) from the product, and parts of the face sheet and core were cut off. Because it is difficult to remove the core at the upper fixed part, a part of the core was fixed together. A shear force was applied using a tensile tester (Autograph, Shimadzu Corporation), and a load-displacement curve was obtained.

**Fig. 4** Experimental setup for drawing. **a** Dimensions of drawing die [mm], **b** Under examination
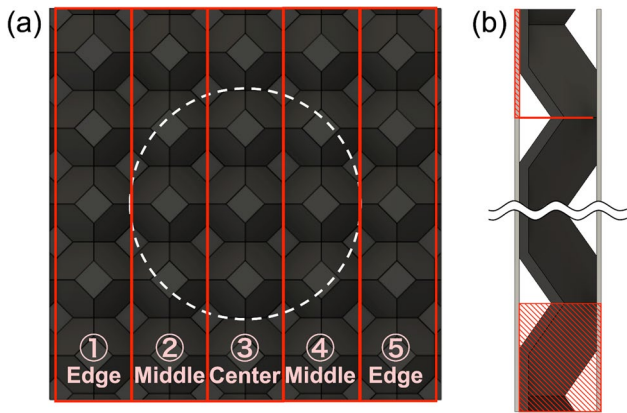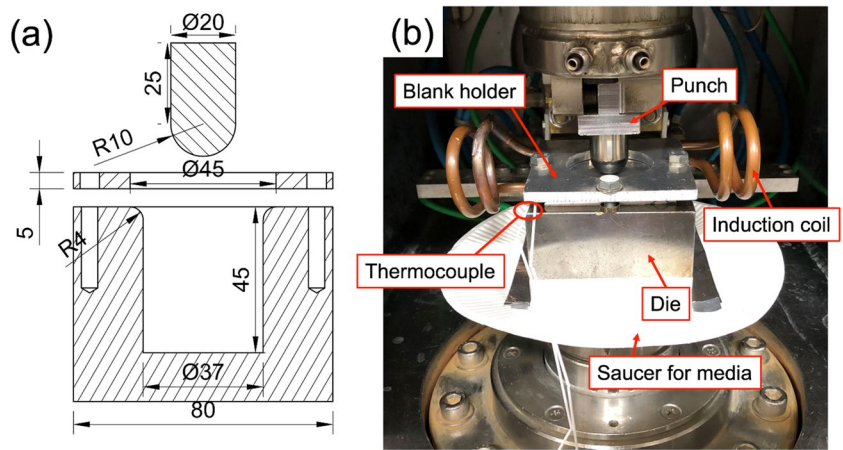




**Fig. 5** Shear strength test. **a** Cut out from drawing specimen, **b** Specimen for tensile test

The dashed white line represents the drawn area. Cut along the red line to remove the shaded area so that a shear load was applied.

## Results

Figure 6 shows the appearance of the specimens after drawing with ice, wax, and a fusible alloy. Compared to the images on the left in Fig. 2, wrinkles and buckling are drastically suppressed. The height of the drawn sheets, drawing stroke, and top thickness are summarized in Table 2.

The applied punch strokes, which were determined in advance of the experiments, were 20 mm for ice and 15 mm for wax and fusible alloys. Figure 7 shows the load-stroke curve during forming.

The difference in the load magnitude corresponded to the difference in the material stiffness of the encapsulated media. The sheets filled with ice and wax had a

**Fig. 6** Specimens after drawing. **a** Filled with ice, **b** Filled with wax, **c** Filled with fusible alloy
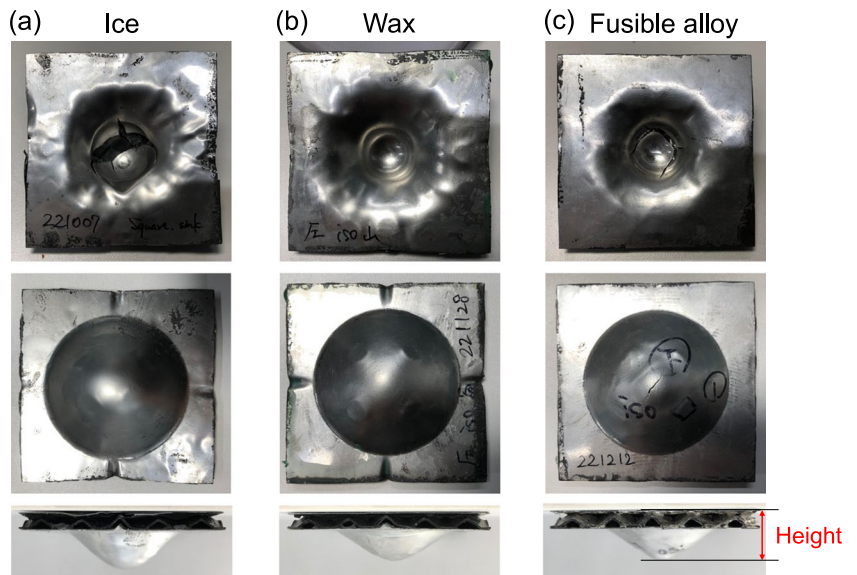
**Table 2** Height of the drawing

|  | Ice | Wax | Fusible alloy |
|---|---|---|---|
| Height [mm] | 21.4 | 17.0 | 18.1 |
| Stroke [mm] | 20 | 15 | 15 |
| Thickness [mm] | 1.4 | 2.0 | 3.1 |
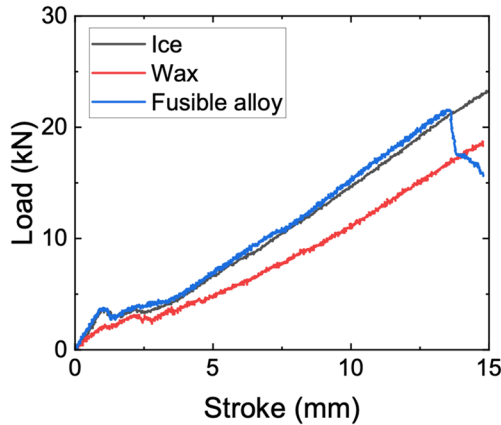


**Fig. 7** Load-stroke curve during drawing



**Fig. 8** Load-displacement curve during shear strength test

**Table 3** Maximum shear load and stress

|  |  | Edge | Middle |
|---|---|---|---|
| Shear load at break [N] |  | 608 | 251 |
| Shear stress at break [N/mm$^2$] | Apparent | 1.06 | 0.44 |
|  | Practical | 8.09 | 3.34 |

wrinkle-free drawing area, although slight wrinkling occurred at the edge where the constraint was weak because the encapsulated media protruded from the specimen. The sheet filled with the fusible alloy had no wrinkles, including around the drawn area; however, the face sheet cracked at a stroke of 13.6 mm, as shown in Figs. 6 and 7. The Ericksen value of stainless steel is 13 mm, although it depends on grain size [19]. This suggests that owing to the hydrostatic effect of the encapsulated media, the drawing limit of monolithic stainless steel could also be attained in the sandwich sheet without wrinkles or forming defects. The rhombus-shaped dome cores, which are shown in the center and right of Fig. 2, were similarly drawable without wrinkles, although they were anisotropic and more likely to have wrinkles.

The load-displacement curve of the shear strength tests of the specimens after drawing with the fusible alloy is shown in Fig. 8. Specimen 3 in the center was severely damaged and could not be subjected to a shear test.

The deformation with a small reaction force at the initial stage of deformation and large fracture displacement of the specimens of the middle sections are caused by the stretching of the domed test piece. Based on ISO 4587 [20], the shear strength was evaluated using the maximum load at break and is summarized in Table 3. Two types of adhesion areas, the apparent area of the test piece (576 mm$^2$) and practically bonded area (75.1 mm$^2$), were used. The load decreased step-by-step owing to the intermittent breakage
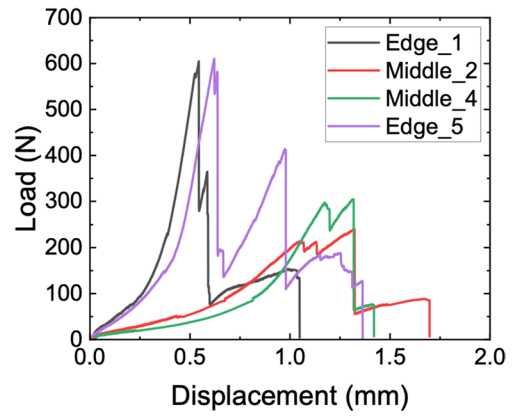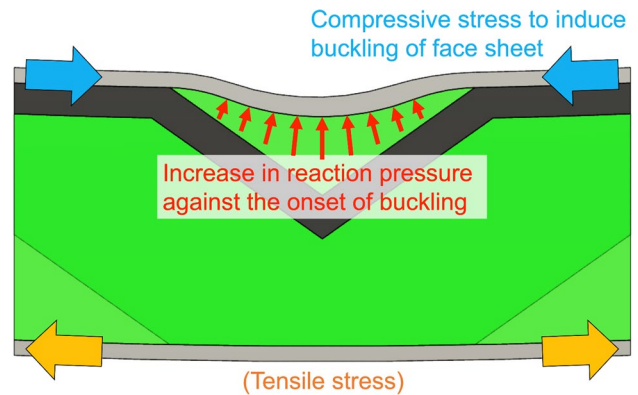


**Fig. 9** Mechanism of suppressing wrinkles

of the scattered bonding surface. The load at the first drop was adopted and the two results were averaged.

## Discussion

The main reason for the absence of wrinkles is that the deformation of the face sheet was restricted by the hydrostatic effects of the encapsulated media, as shown in Fig. 9.

A face sheet subjected to compressive bending stress generated during drawing tended to buckle. The buckling direction was inward, because it was bent in the former phase. The encapsulated media compressed by the initiation of

buckling generated a reaction pressure that suppresses the buckling of the face sheet. As a thin face sheet generates only a small force, the reaction pressure transcends it.

Other factors also contribute to the suppression of wrinkles. By encapsulating robust materials compared to thin cores, the non-uniformity of properties in the face sheet owing to scattered adhesion to the core was mitigated.

Moreover, encapsulated media are brittle and break easily under tensile stress. This characteristic reduces the deformation on the compression side, and the buckling of the face sheet is less likely to occur.

The occurrence of cracks when filled with fusible alloy was caused by the increase in bending stress because the decrease in thickness was smaller than that in other media owing to its hardness, as listed in Table 2.

Observation of the cross-section of the specimens, which is shown in Fig. 10, shows that the fracture of the core could not be perfectly suppressed for both encapsulated media.

The first load drop in the load-displacement curve in Fig. 7 represents this failure, which occurred at a displacement of approximately 2 mm. Based on the maximum shear load summarized in Table 3, if no fracture occurred in the edge portion where the deformation was extremely small, the middle region had 59% adhesive failure. The brittleness of the core causes this fracture, which can be mitigated by changing it to ductile materials. However, it is very valuable to make it possible to form sandwich sheets without buckling and wrinkles and not to deteriorate its properties, as illustrated by the smooth load-displacement curve in Fig. 7.

Differences in the properties of the encapsulated media affected their formability and removability. Ice was advantageous in that it could be melted and removed easily by leaving the test piece at room temperature as shown in Fig. 10a. However, it should be treated at a low temperature during forming, and temperature control is difficult compared with other encapsulated media. When ice heats up, it melts or softens, and cannot maintain the hardness to restrict wrinkles. Wax exhibited a slightly large displacement at the initial load drop. As listed in Table 4, wax is softer than the other materials. Therefore, the core can move freely and deform during forming.

The fusible alloy had no wrinkles also around the drawing area. In the case of industry, there are cases where only the drawn portion is used as a product, and cases where a

**Table 4** Vickers hardness of encapsulated media

|  | Ice (-20 °C) [21] | Wax | Fusible alloy |
|---|---|---|---|
| Vickers hardness [kg/mm$^2$] | 6.0 (Depends on loading time) | 2.25 | 14.0 |

portion of a large flat plate is drawn and used as a whole. In the latter case, a fusible alloy would be suitable. Among the media used in this study, a fusible alloy that can be deformed while maintaining sheet thickness was the best.

Regarding ease of removal, waxes and fusible alloys were left in the sandwich sheets even after they are melted away. This is due to the high viscosity and surface tension, respectively. Ice is the best of the three for removal.

To find better material for encapsulated media, the properties required are summarized as follows:

(i)   The hardness is sufficient to constrain the deformation of the face sheet.
(ii)  Softness that does not hinder the core deformation.
(iii) A low melting point capable of melt filling without damaging the core.
(iv)  A melting point that does not require cooling during molding.
(v)   Easy removal performance (fluidity, volatility, and surface tension).

(i) and (ii) exhibit contradictory results. Because (i) has the highest priority, it is realistic to use the softest one to satisfy (i). According to requirements (iii) and (iv), the suitable melting point is between room temperature and 200 °C. (v) is an independent property, and there is a possibility that an excellent medium can be found by considering methods that are not limited to melting and natural flow, such as chemical processing.

# Conclusion

By extending the freeze-bend method to the secondary formation of sandwich sheets and filling the sandwich sheet with encapsulated media during drawing, it was possible to

**Fig. 10** Cross-sectional image through the center. **a** Filled with ice, **b** Filled with fusible alloy

(a) (b)
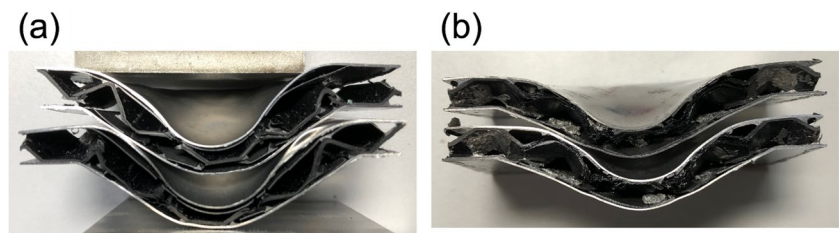
mold without causing wrinkles, which is the forming defect of sandwich sheets with a 3D core and thin face sheets. The reaction pressure generated by the encapsulated media functioned as a buckling-suppression mechanism. Although the cores were fractured because of the ductility of the core material, forming without wrinkles could be attained.

The main aim of this research is, as the first step, the proposal of the novel forming process of the sandwich sheets, which are made of face sheet and 3D core. More detailed investigation in the optimized process parameters must be performed in future, e.g. by changing the media suitable to keep the 3D shape of the varied core structure of the sandwich sheet.

## Declarations

**Competing interests** The authors declare no conflict of interest.

## References

1. Sun Y, Li C, Wu H, Tan K, Zhang F (2018) Simulation and lightweight design for the structure frame of a flying car. Advances in Intelligent Systems Research Proceedings of the 2018 international conference on computer modeling, simulation and algorithm (CMSA 2018):25–29. https://doi.org/10.2991/cmsa-18.2018.7

2. Zhang W, Xu J (2022) Advanced lightweight materials for automobiles: a review. Mater Des 221:110994. https://doi.org/10.1016/j.matdes.2022.110994

3. Yanagimoto J, Ikeuchi K (2012) Sheet forming process of carbon fiber reinforced plastics for lightweight parts. CIRP Ann Manuf Technol 61(1):247–250. https://doi.org/10.1016/j.cirp.2012.03.129

4. Zhang J, Zhou P, Guan C, Liu TQ, Kang WH, Feng P, Gao S (2021) An ultra-lightweight CFRP beam-string structure. Compos Struct 257:113149. https://doi.org/10.1016/j.compstruct.2020.113149

5. Putnam J, Littell J (2019) Evaluation of impact energy attenuator and composite material designs of a UAM VTOL concept vehicle. Proceeding from the VFS 75th Annual Forum and Technology Display. https://core.ac.uk/works/85881033

6. Zhang J, Yanagimoto J (2021) Topology optimization of microlattice dome with enhanced stiffness and energy absorption for additive manufacturing. Compos Struct 255:112889. https://doi.org/10.1016/j.compstruct.2020.112889

7. Wei P, Li Z, Li X, Wang MY (2018) An 88-line MATLAB code for the parameterized level set method based topology optimization using radial basis functions. Struct Multidisc Optim 58(2):831–849. https://doi.org/10.1007/s00158-018-1904-8

8. Vinson JR (2001) Sandwich structures. Appl Mech Rev 54(3):201–214. https://doi.org/10.1115/1.3097295

9. Heimbs S (2009) Virtual testing of sandwich core structures using dynamic finite element simulations. Comp Mater Sci 45:205–216. https://doi.org/10.1016/j.commatsci.2008.09.017

10. Seong DY, Jung CG, Yang DY, Kim JH, Chung WJ, Lee MY (2010) Bendable metallic sandwich plates with a sheared dimple core. Scr Mater 63(1):81–84. https://doi.org/10.1016/j.scriptamat.2010.03.022

11. Mohr D (2005) On the role of shear strength in sandwich sheet forming. Int J Solids Struct 42(5–6):1491–1512. https://doi.org/10.1016/j.ijsolstr.2004.07.012

12. Daniel IM, Gdoutos EE, Wang K-A, Abot JL (2002) Failure modes of composite sandwich beams. Int J Damage Mech 11:309–334. https://doi.org/10.1106/105678902027247

13. Mohan K, Hon YT, Idapalapati S, Seow HP (2005) Failure of sandwich beams consisting of alumina face sheet and aluminum foam core in bending. Mater Sci Eng A 409(1–2):292–301. https://doi.org/10.1016/j.msea.2005.06.070

14. Xiong J, Ghosh R, Ma L, Ebrahimi H, Hamouda AMS, Vaziri A, Wu L (2014) Bending behavior of lightweight sandwich-walled shells with pyramidal truss cores. Compos Struct 116:793–804. https://doi.org/10.1016/j.compstruct.2014.06.006

15. Bühring J, Nuño M, Schröder KU (2021) Additive manufactured sandwich structures: mechanical characterization and usage potential in small aircraft. Aerosp Sci Technol 111:106548. https://doi.org/10.1016/j.ast.2021.106548

16. Shibuya Y, Zhang J, Sato Y, Yanagimoto J (2022) Enhancement of mechanical property and formability of CFRP core sandwich sheets by additive manufacturing process-induced material and structural anisotropies. J Mater Process Technol 310:117778. https://doi.org/10.1016/j.jmatprotec.2022.117778

17. Tashiro Y, Nakajima T (2003) Development of an energy-conserving bending method for double titanium Pipes. Yamaha motor technical review. https://global.yamaha-motor.com/jp/design_technology/technical/thesis/pdf/browse/37gr_08.pdf

18. Morgan G (1999) Workholding with fusible alloys. Aircr Eng Aerosp Technol 71(6):576–578. https://doi.org/10.1108/00022669910303739

19. Ohashi N, Ono Y, Nohara K (1977) Press formability of stainless steel sheets. Tetsu-To-Hagane 63:812–823. https://doi.org/10.2355/tetsutohagane1955.63.5_812

20. ISO 4587 Adhesives — Determination of tensile lap-shear strength of rigid-to-rigid bonded assemblies (2003). https://www.iso.org/standard/34852.html

21. Bowden FP (1953) Friction on snow and ice. Proc R Soc Lond A 217(1131):462–478. https://doi.org/10.1098/rspa.1953.0074

**Publisher's note** Springer Nature remains neutral with regard to jurisdictional claims in published maps and institutional affiliations.